JACS
JOURNAL OF THE AMERICAN CHEMICAL SOCIETY
pubs.acs.org/JACS
Communication

# Enzyme-Responsive Peptide Thioesters for Targeting Golgi Apparatus

Weiyi Tan, Qiuxin Zhang, Monica C. Quiñones-Frías, Alan Y. Hsu, Yichi Zhang, Avital Rodal, Pengyu Hong, Hongbo R. Luo, and Bing Xu*

Cite This: J. Am. Chem. Soc. 2022, 144, 6709−6713
Read Online
ACCESS | Metrics & More | Article Recommendations | Supporting Information

**ABSTRACT:** The Golgi apparatus (GA) is the hub of intracellular trafficking, but selectively targeting GA remains a challenge. We show an unconventional types of peptide thioesters, consisting of an aminoethyl thioester and acting as substrates of thioesterases, for instantly targeting the GA of cells. The peptide thioesters, above or below their critical micelle concentrations, enter cells mainly via caveolin-mediated endocytosis or macropinocytosis, respectively. After being hydrolyzed by GA-associated thioesterases, the resulting thiopeptides form dimers and accumulate in the GA. After saturating the GA, the thiopeptides are enriched in the endoplasmic reticulum (ER). Their buildup in ER and GA disrupts protein trafficking, thus leading to cell death via multiple pathways. The peptide thioesters target the GA of a wide variety of cells, including human, murine, and *Drosophila* cells. Changing D-diphenylalanine to L-diphenylalanine in the peptide maintains the GA-targeting ability. In addition, targeting GA redirects protein (e.g., NRAS) distribution. This work illustrates a thioesterase-responsive and redox-active molecular platform for targeting the GA and controlling cell fates.



The Golgi apparatus (GA)[1,2] is an important hub for different signaling pathways.[3−5] As an essential component of the secretory pathway used by all eukaryotic cells to distribute membrane and secretory proteins,[6] GA is emerging as important target for understanding and treating illnesses such as cancer[7] and Alzheimer's disease.[8] The increasing understanding of the protein trafficking to and from the GA, such as the sophisticated delivery of proteins from the endoplasmic reticulum (ER) to GA,[9] also highlights a unique opportunity to develop molecules to target the GA for modulating cell functions. Although there are several existing molecular probes for imaging the GA,[10,11] they still require pretreatment,[10] take a relatively long incubation time,[11,12] or only respond to certain cells.[11] Thus, there is still an unmet need to develop molecules for targeting the GA.

Our recent work on thiophosphopeptides instantly targeting the GA and selectively killing cancer cells[13] reveals two important insights: (i) an enzymatic reaction enables instant and efficient GA targeting and (ii) a redox reaction enables the proper thiopeptides to accumulate in the GA of cells by self-assembly, dimerization, and a plausible reaction with cysteine-rich proteins (CRPs). On replacing thiophosphate group with other sulfur-containing moieties, we unexpectedly found that fluorescent peptide thioesters instantly target the GA of a wide variety of cells. Consisting of an aminoethyl thioester as the enzyme-responsive cap at a terminal of self-assembling D-diphenylalanine (ff)[14] and nitrobenzoxadiazole (NBD) as the fluorophore at the other end of ff, the peptide thioesters (**1** and **3**, Scheme 1) fail to undergo an S to N acyl shift[15] of the conventional peptide thioesters used for protein synthesis.[16−18] The peptide thioester (**1** or **3**), above or below its critical micelle concentration (CMC), enters cells mainly via caveolin-mediated endocytosis or macropinocytosis, respectively (Scheme 1). After being hydrolyzed by Golgi-associated thioesterases, such as PPT1,[19] LYPLA1,[20] and LYPLA2,[21] the resulting thiopeptide (**2** or **4**) (Scheme 1 and Scheme S4) forms dimers and likely reacts with CRPs in GA, thus accumulating in the GA. After they saturate the GA, the peptide thiols are enriched in the ER. At about 5−10 times of the concentrations used for imaging the GA, the peptide thioesters build up in the ER and GA, resulting in ER stress, and disrupt protein trafficking (e.g., NRAS trafficking), thus resulting in cell death via multiple pathways. While changing ff to L-diphenylalanine (FF) maintains the GA-targeting ability of the peptide thioester (**5**), additional controls (**7**−**13**, Scheme S5), such as replacing the thioester by methylsulfonyl group or thioether, switching the thioester to a carboxyl ester or amide, or mutating the D-phenylalanine to D-alanine, fail to target the GA. **1** instantly targets the GA of a variety of cells, including human, murine, and *Drosophila* cells. In addition, **1** redirects the distribution of NRAS. This work illustrates an unconventional type of self-assembling peptide thioesters as a new and facile molecular platform for targeting the GA and controlling cell fates via enzymatic activation and redox reactions in cells.

**1** instantly enters the cells, and the fluorescence resulting from **1** overlaps with that of Golgi-RFP (Figure 1A). Fluorescence appears in the cytosolic region and at the GA immediately after the addition of **1**, and the GA becomes

**Received:** February 27, 2022
**Published:** April 11, 2022

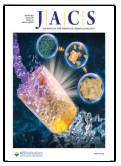




https://doi.org/10.1021/jacs.2c02238
J. Am. Chem. Soc. 2022, 144, 6709−6713

**Scheme 1. Enzyme-Responsive Peptide Thioesters Targeting GAs**

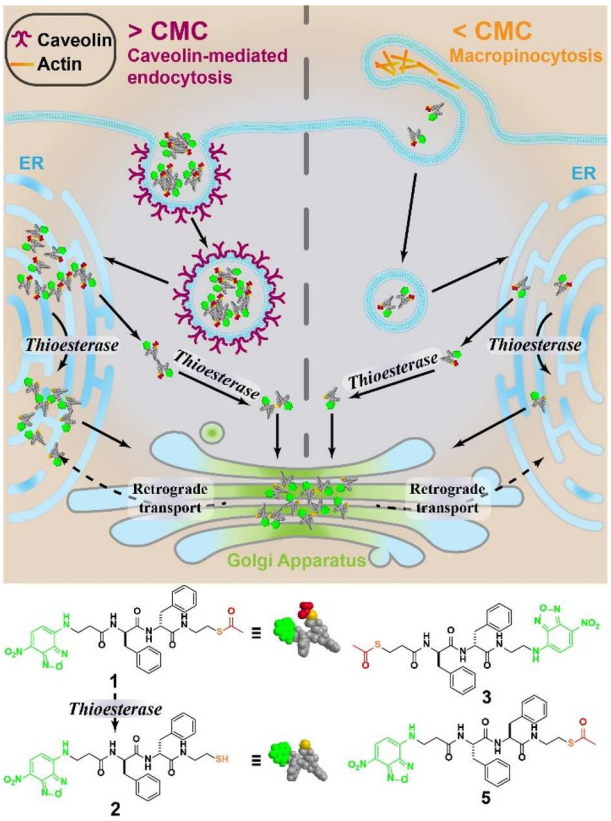


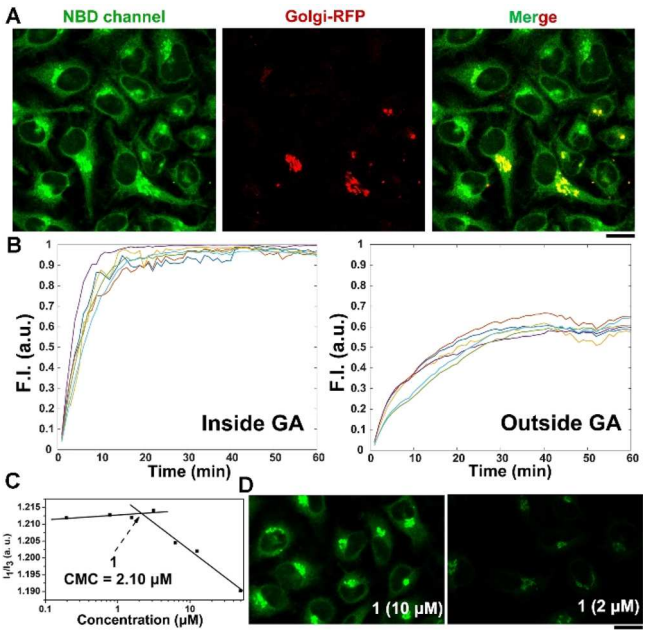


**Figure 1.** (A) CLSM of Golgi-RFP transfected HeLa treated with **1** (10 $\mu$M, 30 min). (B) Single-cell analysis of fluorescence inside and outside the GA of HeLa treated with **1** (10 $\mu$M, 60 min). (C) CMC of **1**. (D) CLSM of HeLa treated with **1** (10 or 2 $\mu$M) for 30 min (scale bar 20 $\mu$m).

distinguishable in less than 1 min (Figures S1 and S2 and Video S1). A single-cell imaging analysis (Figure 1B) confirms a faster fluorescence increase inside rather than outside the GA: the fluorescence plateaus in less than 15 min or for longer than 45 min at the GA or outside the GA, respectively, and the plateaus of the fluorescence are higher at the GA in comparison to those outside the GA. An LC/MS analysis of the lysate of HeLa cells incubated with **1** for 24 h reveals that about 60% of the peptide thioester (**1**) turns into the corresponding thiol (**2**) and around 55% of **2** forms a dimer (Figure S3). The dimers, resulting from intracellular oxidants that oxidize **2**, enhance the accumulation of **2** at the GA. These results indicate that **1**, being deacetylated to give **2**, accumulates primarily at the GA.

**1** enters HeLa cells differently below and above its critical micelle concentration (CMC = 2.1 $\mu$M, Figure 1C). m$\beta$CD,[22] a caveolin-mediated endocytosis (CME) inhibitor, significantly slows down the fluorescence buildup at the GA of the cell treated with 10 $\mu$M of **1**; CytD,[23] a macropinocytosis inhibitor, dramatically decreases the fluorescence at GA of the cells incubated with 2 $\mu$M of **1** (Figure S4). Single-cell analyses (Figures S5−S7) confirm that m$\beta$CD is more potent at inhibiting the GA accumulation in comparison to CytD when HeLa cells are treated with 10 $\mu$M of **1**, while CytD is more potent in the case of 2 $\mu$M of **1**. Treating the HeLa cells with chlorpromazine suggests that **1** hardly or only slightly depends on clathrin-mediated endocytosis (Figure S8) at 2 and 10 $\mu$M, respectively. These results suggest that the assemblies and monomers of **1** enter cells mainly via CME and macropinocytosis, respectively.

Thioesterase inhibitors, ML211[24−26] and DC661,[27] by themselves or in combination, efficiently block **1** accumulating at the GA (Figures S4, S9, and S10). Meanwhile, neither inhibitor can block the GA accumulation of a commercial Golgi dye, C6-NBD-Ceramide[28] (Figures S11 and S12). However, carboxylesterase (CES1) is able to catalyze the hydrolysis of **1** in a cell-free assay (Figure S13) and pretreating HeLa cells with the nonspecific esterase inhibitor bis(*p*-nitrophenyl) phosphate[29] hardly decreases the rate of fluorescence increase from **1** at the GA (Figure S14). These results suggest that thioesterases (i.e., LYPLA1, LYPLA2, and PPT1) contribute to the deacetylation of **1** to form **2** and act as a main control for **1** to target GA.

Fluorescence appears instantly inside cells in less than 1 min after adding **1** in the culture of HeLa cells (Figure 2A). The fluorescence at GA increases significantly with the time of incubation of **1**, and the GA can be easily distinguished from the background in less than 4 min (Figure 2A). There is at least a 3 times enhancement of the fluorescence intensity at GA from 1 to 8 min (Figure S15). The fluorescence outside the GA increases significantly after 16 min, likely due to the retrograde Golgi to ER trafficking.[30] While C6-NBD-ceramide[28] shows dim fluorescence over 16 min (Figure S16), **1** exhibits a superior ability for targeting the GA. Unlike the thiophosphopeptide,[13] **1** is able to target the GA of various cells from different organisms (Figure 2B), such as *Homo sapiens* (HeLa, Saos-2, HEK293, MCF-7, HS-5, SJSA-1, and HepG2), *Mus musculus* (B16F10), and *Drosophila* (S2). Single-cell analyses of fluorescence at the GA (Figure S17) and CLSM images (Figures S18−S23) of different cell lines confirm that **1** accumulates at the GA of these cells swiftly. **1** also rapidly enters primary cells, such as neutrophils (polymorphonuclear leukocytes), and localizes at the GA (Figure S24). These results establish that **1** is able to target the GA of a wide variety of cells, likely due to the fact that thioesterases are essential and ubiquitous.[31]



https://doi.org/10.1021/jacs.2c02238
J. Am. Chem. Soc. 2022, 144, 6709−6713

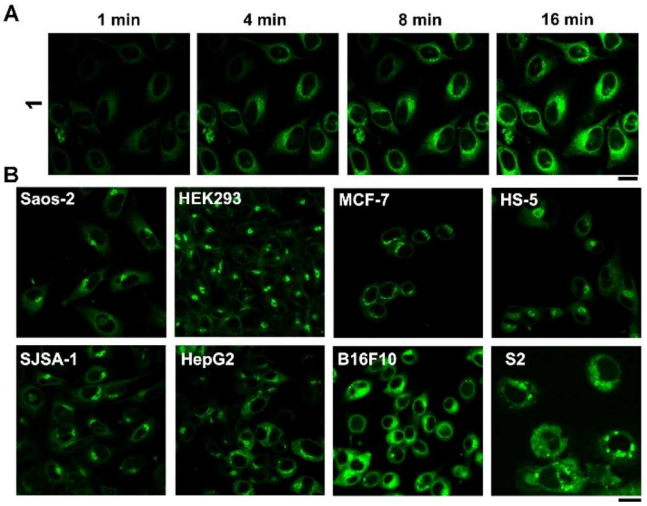


**Figure 2.** CLSM images of (A) HeLa treated with **1** for 1, 4, 8, and 16 min and (B) different cells (Saos-2, HEK293, MCF-7, HS-5, SJSA-1, HepG2, B16F10, and S2) treated with **1** for 8 min ([**1**] = 10 $\mu$M, scale bar 20 $\mu$m).

Above 20 $\mu$M, **1** significantly inhibits HeLa, HEK293, Saos-2, MCF-7, and HS-5 cells (Figure 3A) with $IC_{50}$ values of 15.0,

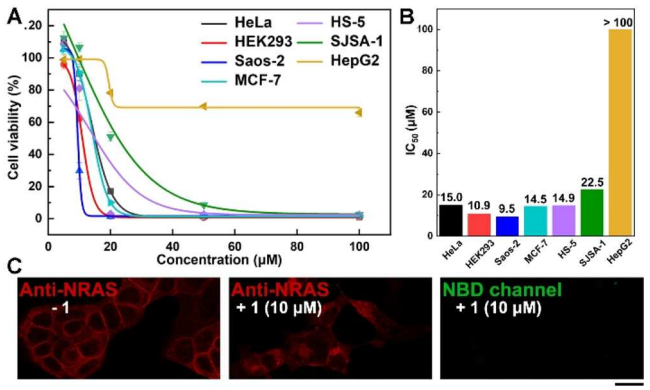


**Figure 3.** (A) Cytotoxicity and (B) $IC_{50}$ of **1** against different cell lines (HeLa, HEK293, Saos-2, MCF-7, HS-5, SJSA-1, and HepG2). (C) ICC staining of MCF-7 with NRAS antibody after pretreatment with or without **1** (10 $\mu$M, 30 min; scale bar 20 $\mu$m).

10.9, 9.5, 14.5, and 14.9 $\mu$M, respectively. Several commonly used inhibitors (Z-VAD-FMK, NAc, Nec-1, DFO, disulfiram, and PD150606)[32] of cell death hardly rescue these four cell lines (Figure S25), indicating that **1** results in cell death via multiple pathways or possibly a new mechanism. **1** shows slightly mild cytotoxicity against SJSA-1 cells ($IC_{50}$ = 22.5 $\mu$M) and exhibits a rather low inhibitory activity against HepG2 cells, with $IC_{50}$ values of above 100 $\mu$M (Figure 3B). These results coincide with the high level of glutathione (GSH) in hepatocytes[33] and in SJSA-1,[34] as GSH compromises the cytotoxicity of the redox-active **2**. Depletion of GSH in HepG2 cells by L-buthionine-sulfoximine (BSO)[35] significantly increases the cytotoxicity of **1** against HepG2 cells ($IC_{50}$ drops to 13.45 $\mu$M; Figure S26), which supports the notion that GSH antagonizes the peptide thioesters.

Because the trafficking of oncogenic NRAS between the GA and plasma membrane is essential for tumor growth,[36] we determined the intracellular distribution of NRAS of MCF-7 cells. NRAS, being overexpressed in MCF-7,[37] relocates from mainly the plasma membrane to overwhelmingly the GA after the pretreatment of **1** for 30 min (Figure 3C left and middle). No fluorescence in the NBD channel (green, Figure 3C) after the standard immunocytochemistry staining excludes the notion that the redistribution of NRAS is due to bleed-through. As S-palmitoylation is a critical process for protein trafficking,[38] this result suggests that **1** disrupts GA functions and interferes with the secretory pathway, which likely contributes to its cytotoxicity when the accumulation of **1** at GA reaches a certain threshold.

**3**, behaving similarly to **1**, enters cells in a concentration-dependent manner (Figures S27−S29) and swiftly accumulates at the GA (Figure S30A and Video S2). Thioesterase inhibitors slow the GA accumulation of **3** (Figures S31 and S32). The cytotoxicity of **3** is slightly lower than that of **1**, but with a similar trend (Figure S30B), indicating that (i) the acetyl thioester is enzyme-responsive on either the C- or N-terminal of the peptide thioester and (ii) **1** and **3** likely enter and accumulate at GA via similar mechanisms. **5**, having FF instead of ff, accumulates at the GA at a rate similar to that of **1** (Figures S30A and S33 and Video S3). These results suggest that the cellular uptake of **1**, **3**, or **5** and the rapid GA accumulation of **2**, **4**, or **6** depend instead on the enzyme response of the thioester group rather than on their configurations. The cytotoxicity of **5** is much lower than that of **1** (Figure S30B), in agreement with the proteolysis of **5**. On replacement of the thioester with a methylsulfonyl group or a methyl thioether, respectively (Scheme S5), there is resistance to enzymatic cleavage (Figure S34) and **7** or **8** fails to accumulate at the GA (Figures S35−S37). Analogues with the thioester being replaced with an ester (**9**) or amide (**10**) (Scheme S5) are unable to accumulate at the GA (Figures S35, S38, and S39). Although cells cleave the ester bond of **9** (Figure S40A), there is little fluorescence at the GA, confirming that a redox-active thiol is crucial for GA targeting. When D-dialanine replaces diphenylalanine (**11**; Scheme S5), though **11** is enzymatically responsive (Figure S40B), it hardly enters cells and accumulates at the GA (Figures S35 and S41). When the ff motif is omitted from **1** (**12**; Scheme S5) **12** exhibits the intracellular behavior similar to that of **11**, not targeting the GA (Figures S35, S41, and S42). TEM shows that **11** hardly self-assembles while **1** self-assembles into nanoparticles and nanofibers at 20 $\mu$M (Figure S43). These results indicate that self-assembly is essential for the peptide thioesters to target the GA. **13**, with a thioester on a cysteine residue (Scheme S5) as the enzymatically responsive thioester bond (Figure S40C), fails to target the GA (Figures S35 and S44). **7**−**13** exhibits low cytotoxicity against HeLa cells (Figure S30C), in agreement with their inability to target the GA.

In summary, this work illustrates that several peptide thioesters undergo enzymatic hydrolysis and instantly accumulate at the GA. Although **2** also accumulates slowly at the GA,[13] the thioester group, acting as a preform of thiol and one type of high-energy bond *in vivo*,[39] is a unique and useful building block for an enzymatic response. This instant GA-targeting process not only allows the imaging of ER and GA trafficking[40] but also provides new insights into developing supramolecular assemblies[41−44] for disrupting protein trafficking and further controlling cell fates. Although the detailed mechanism remains to be further elucidated, dimerization of the thiopeptides and the likely reaction with CRPs in GA[45] contribute to the GA accumulation, providing a new way for modulating GA signaling cascades.



https://doi.org/10.1021/jacs.2c02238
J. Am. Chem. Soc. 2022, 144, 6709−6713

## ■ ASSOCIATED CONTENT

### Supporting Information

The Supporting Information is available free of charge at https://pubs.acs.org/doi/10.1021/jacs.2c02238.

Materials and detailed experimental procedures, TEM and CLSM images, cell viabilities, LC/MS spectra, and chemical structures of the compounds (PDF)

**1** (10 $\mu$M) incubated with HeLa cells over 30 min (AVI)

**3** (10 $\mu$M) incubated with HeLa cells over 30 min (AVI)

**5** (10 $\mu$M) incubated with HeLa cells over 30 min (AVI)

## ■ AUTHOR INFORMATION


### Corresponding Author

**Bing Xu** − *Department of Chemistry, Brandeis University, Waltham, Massachusetts 02453, United States;* orcid.org/0000-0002-4639-387X; Email: bxu@brandeis.edu

### Authors

**Weiyi Tan** − *Department of Chemistry, Brandeis University, Waltham, Massachusetts 02453, United States;* orcid.org/0000-0001-5316-8278

**Qiuxin Zhang** − *Department of Chemistry, Brandeis University, Waltham, Massachusetts 02453, United States*

**Monica C. Quiñones-Frías** − *Department of Biology, Brandeis University, Waltham, Massachusetts 02453, United States*

**Alan Y. Hsu** − *Department of Pathology, Harvard Medical School and Department of Laboratory Medicine, Children's Hospital Boston and Dana-Farber/Harvard Cancer Center, Boston, Massachusetts 02115, United States;* orcid.org/0000-0001-5680-345X

**Yichi Zhang** − *Department of Chemistry, Brandeis University, Waltham, Massachusetts 02453, United States*

**Avital Rodal** − *Department of Biology, Brandeis University, Waltham, Massachusetts 02453, United States*

**Pengyu Hong** − *Department of Computer Science, Brandeis University, Waltham, Massachusetts 02453, United States*

**Hongbo R. Luo** − *Department of Pathology, Harvard Medical School and Department of Laboratory Medicine, Children's Hospital Boston and Dana-Farber/Harvard Cancer Center, Boston, Massachusetts 02115, United States*

Complete contact information is available at: https://pubs.acs.org/10.1021/jacs.2c02238


### Notes

The authors declare no competing financial interest.

## ■ ACKNOWLEDGMENTS

This work was partially supported by NIH (CA142746, AI141386) and NSF (DMR-2011846 and OAC1920147).

## ■ REFERENCES


(1) Kulkarni-Gosavi, P.; Makhoul, C.; Gleeson, P. A. Form and function of the Golgi apparatus: scaffolds, cytoskeleton and signalling. *FEBS Lett.* **2019**, *593*, 2289−2305.

(2) Lee, M. C.; Miller, E. A.; Goldberg, J.; Orci, L.; Schekman, R. Bi-directional protein transport between the ER and Golgi. *Annu. Rev. Cell Dev. Biol.* **2004**, *20*, 87−123.

(3) Bivona, T. G.; Pérez de Castro, I.; Ahearn, I. M.; Grana, T. M.; Chiu, V. K.; Lockyer, P. J.; Cullen, P. J.; Pellicer, A.; Cox, A. D.; Philips, M. R. Phospholipase C$\gamma$ activates Ras on the Golgi apparatus by means of RasGRP1. *Nature* **2003**, *424*, 694−698.

(4) Farber-Katz, S. E.; Dippold, H. C.; Buschman, M. D.; Peterman, M. C.; Xing, M.; Noakes, C. J.; Tat, J.; Ng, M. M.; Rahajeng, J.; Cowan, D. M.; Fuchs, G. J.; Zhou, H.; Field, S. J. DNA damage triggers golgi dispersal via DNA-PK and GOLPH3. *Cell* **2014**, *156*, 413−427.

(5) Rieger, L.; O'Shea, S.; Godsmark, G.; Stanicka, J.; Kelly, G.; O'Connor, R. IGF-1 receptor activity in the Golgi of migratory cancer cells depends on adhesion-dependent phosphorylation of Tyr1250 and Tyr1251. *Sci. Signal.* **2020**, *13*, No. eaba3176.

(6) Barlowe, C.; Helenius, A. Cargo Capture and Bulk Flow in the Early Secretory Pathway. *Annu. Rev. Cell Dev. Biol.* **2016**, *32*, 197−222.

(7) Wlodkowic, D.; Skommer, J.; McGuinness, D.; Hillier, C.; Darzynkiewicz, Z. ER-Golgi network-A future target for anti-cancer therapy. *Leukemia Res.* **2009**, *33*, 1440−1447.

(8) Joshi, G.; Chi, Y.; Huang, Z.; Wang, Y. A$\beta$-induced Golgi fragmentation in Alzheimer's disease enhances A$\beta$ production. *Proc. Natl. Acad. Sci. U.S.A.* **2014**, *111*, E1230−E1239.

(9) Weigel, A. V.; Chang, C.-L.; Shtengel, G.; Xu, C. S.; Hoffman, D. P.; Freeman, M.; Iyer, N.; Aaron, J.; Khuon, S.; Bogovic, J.; Qiu, W.; Hess, H. F.; Lippincott-Schwartz, J. ER-to-Golgi protein delivery through an interwoven, tubular network extending from ER. *Cell* **2021**, *184*, 2412−2429.

(10) van Echten-Deckert, G.; Giannis, A.; Schwarz, A.; Futerman, A. H.; Sandhoff, K. 1-Methylthiodihydroceramide, a novel analog of dihydroceramide, stimulates sphinganine degradation resulting in decreased de novo sphingolipid biosynthesis. *J. Biol. Chem.* **1998**, *273*, 1184−91.

(11) Zhang, H.; Fan, J.; Wang, J.; Zhang, S.; Dou, B.; Peng, X. An off−on Cox-2-specific fluorescent probe: Targeting the golgi apparatus of cancer cells. *J. Am. Chem. Soc.* **2013**, *135*, 11663−11669.

(12) Hu, X.; Hai, Z.; Wu, C.; Zhan, W.; Liang, G. A Golgi-Targeting and Dual-Color "Turn-On" Probe for Spatially Precise Imaging of Furin. *Anal. Chem.* **2021**, *93*, 1636−1642.

(13) Tan, W.; Zhang, Q.; Wang, J.; Yi, M.; He, H.; Xu, B. Enzymatic Assemblies of Thiophosphopeptides Instantly Target Golgi Apparatus and Selectively Kill Cancer Cells. *Angew. Chem., Int. Ed.* **2021**, *60*, 12796−12801.

(14) Reches, M.; Gazit, E. Casting Metal Nanowires Within Discrete Self-Assembled Peptide Nanotubes. *Science* **2003**, *300*, 625−627.

(15) Dang, B.; Kubota, T.; Mandal, K.; Bezanilla, F.; Kent, S. B. H. Native Chemical Ligation at Asx-Cys, Glx-Cys: Chemical Synthesis and High-Resolution X-ray Structure of ShK Toxin by Racemic Protein Crystallography. *J. Am. Chem. Soc.* **2013**, *135*, 11911−11919.

(16) Canne, L. E.; Bark, S. J.; Kent, S. B. H. Extending the Applicability of Native Chemical Ligation. *J. Am. Chem. Soc.* **1996**, *118*, 5891−5896.

(17) Blanco-Canosa, J. B.; Nardone, B.; Albericio, F.; Dawson, P. E. Chemical Protein Synthesis Using a Second-Generation N-Acylurea Linker for the Preparation of Peptide-Thioester Precursors. *J. Am. Chem. Soc.* **2015**, *137*, 7197−7209.

(18) Asahina, Y.; Komiya, S.; Ohagi, A.; Fujimoto, R.; Tamagaki, H.; Nakagawa, K.; Sato, T.; Akira, S.; Takao, T.; Ishii, A.; Nakahara, Y.; Hojo, H. Chemical Synthesis of O-Glycosylated Human Interleukin-2 by the Reverse Polarity Protection Strategy. *Angew. Chem., Int. Ed.* **2015**, *54*, 8226−8230.

(19) Camp, L. A.; Verkruyse, L. A.; Afendis, S. J.; Slaughter, C. A.; Hofmann, S. L. Molecular cloning and expression of palmitoyl-protein thioesterase. *J. Biol. Chem.* **1994**, *269*, 23212−23219.

(20) Duncan, J. A.; Gilman, A. G. A cytoplasmic acyl-protein thioesterase that removes palmitate from G protein $\alpha$ subunits and p21RAS. *J. Biol. Chem.* **1998**, *273*, 15830−15837.

(21) Toyoda, T.; Sugimoto, H.; Yamashita, S. Sequence, expression in Escherichia coli, and characterization of lysophospholipase II. *Biochim. Biophys. Acta. Mol. Cell. Biol. Lipids* **1999**, *1437*, 182−193.

(22) Rodal, S. K.; Skretting, G.; Garred, Ø.; Vilhardt, F.; Deurs, B. v.; Sandvig, K. Extraction of Cholesterol with Methyl-$\beta$-Cyclodextrin Perturbs Formation of Clathrin-coated Endocytic Vesicles. *Mol. Biol. Cell* **1999**, *10*, 961−974.

(23) Lamaze, C.; Fujimoto, L. M.; Yin, H. L.; Schmid, S. L. The actin cytoskeleton is required for receptor-mediated endocytosis in mammalian cells. *J. Biol. Chem.* **1997**, *272*, 20332−20335.
(24) Singha, P. K.; Mäklin, K.; Vihavainen, T.; Laitinen, T.; Nevalainen, T. J.; Patil, M. R.; Tonduru, A. K.; Poso, A.; Laitinen, J. T.; Savinainen, J. R. Evaluation of FASN inhibitors by a versatile toolkit reveals differences in pharmacology between human and rodent FASN preparations and in antiproliferative efficacy in vitro vs. in situ in human cancer cells. *Eur. J. Pharm. Sci.* **2020**, *149*, 105321.
(25) Casasanta, M. A.; Yoo, C. C.; Smith, H. B.; Duncan, A. J.; Cochrane, K.; Varano, A. C.; Allen-Vercoe, E.; Slade, D. J. A chemical and biological toolbox for Type Vd secretion: Characterization of the phospholipase A1 autotransporter FplA from Fusobacterium nucleatum. *J. Biol. Chem.* **2017**, *292*, 20240−20254.
(26) Hernandez, J. L.; Davda, D.; Cheung See Kit, M.; Majmudar, J. D.; Won, S. J.; Gang, M.; Pasupuleti, S. C.; Choi, A. I.; Bartkowiak, C. M.; Martin, B. R. APT2 Inhibition Restores Scribble Localization and S-Palmitoylation in Snail-Transformed Cells. *Cell Chem. Biol.* **2017**, *24*, 87−97.
(27) Rebecca, V. W.; Nicastri, M. C.; Fennelly, C.; Chude, C. I.; Barber-Rotenberg, J. S.; Ronghe, A.; McAfee, Q.; McLaughlin, N. P.; Zhang, G.; Goldman, A. R.; Ojha, R.; Piao, S.; Noguera-Ortega, E.; Martorella, A.; Alicea, G. M.; Lee, J. J.; Schuchter, L. M.; Xu, X.; Herlyn, M.; Marmorstein, R.; Gimotty, P. A.; Speicher, D. W.; Winkler, J. D.; Amaravadi, R. K. PPT1 Promotes Tumor Growth and Is the Molecular Target of Chloroquine Derivatives in Cancer. *Cancer Discovery* **2019**, *9*, 220−229.
(28) Paul, P.; Kamisaka, Y.; Marks, D. L.; Pagano, R. E. Purification and Characterization of UDP-glucose:Ceramide Glucosyltransferase from Rat Liver Golgi Membranes. *J. Biol. Chem.* **1996**, *271*, 2287−2293.
(29) Heymann, E.; Krisch, K.; Büch, H.; Buzello, W. Inhibition of phenacetin- and acetanilide-induced methemoglobinemia in the rat by the carboxylesterase inhibitor Bis-[p-nitrophenyl] phosphate. *Biochem. Pharmacol.* **1969**, *18*, 801−811.
(30) Lee, M. C. S.; Miller, E. A.; Goldberg, J.; Orci, L.; Schekman, R. Bi-directional protein transport between the ER and Golgi. *Annu. Rev. Cell Dev. Biol.* **2004**, *20*, 87−123.
(31) Cantu, D. C.; Chen, Y.; Reilly, P. J. Thioesterases: A new perspective based on their primary and tertiary structures. *Protein Sci.* **2010**, *19*, 1281−1295.
(32) Tang, D.; Kang, R.; Berghe, T. V.; Vandenabeele, P.; Kroemer, G. The molecular machinery of regulated cell death. *Cell Res.* **2019**, *29*, 347−364.
(33) Kretzschmar, M. Regulation of hepatic glutathione metabolism and its role in hepatotoxicity. *Exp. Toxicol. Pathol.* **1996**, *48*, 439−446.
(34) Su, L.; Li, R.; Khan, S.; Clanton, R.; Zhang, F.; Lin, Y.-N.; Song, Y.; Wang, H.; Fan, J.; Hernandez, S.; Butters, A. S.; Akabani, G.; MacLoughlin, R.; Smolen, J.; Wooley, K. L. Chemical Design of Both a Glutathione-Sensitive Dimeric Drug Guest and a Glucose-Derived Nanocarrier Host to Achieve Enhanced Osteosarcoma Lung Metastatic Anticancer Selectivity. *J. Am. Chem. Soc.* **2018**, *140*, 1438−1446.
(35) Romero, F. J.; Sies, H. Subcellular glutathione contents in isolated hepatocytes treated with L-buthionine sulfoximine. *Biochem. Biophys. Res. Commun.* **1984**, *123*, 1116−1121.
(36) Ko, P.-J.; Dixon, S. J. Protein palmitoylation and cancer. *Embo. Rep.* **2018**, *19*, No. e46666.
(37) Graham, K. A.; Richardson, C. L.; Minden, M. D.; Trent, J. M.; Buick, R. N. Varying Degrees of Amplification of the N-*RAS* Oncogene in the Human Breast Cancer Cell Line MCF-7. *Cancer Res.* **1985**, *45*, 2201−2205.
(38) Rocks, O.; Gerauer, M.; Vartak, N.; Koch, S.; Huang, Z.-P.; Pechlivanis, M.; Kuhlmann, J.; Brunsveld, L.; Chandra, A.; Ellinger, B.; et al. The palmitoylation machinery is a spatially organizing system for peripheral membrane proteins. *Cell* **2010**, *141*, 458−471.
(39) Goldford, J. E.; Hartman, H.; Smith, T. F.; Segrè, D. Remnants of an Ancient Metabolism without Phosphate. *Cell* **2017**, *168*, 1126−1134.
(40) Tamura, T.; Fujisawa, A.; Tsuchiya, M.; Shen, Y.; Nagao, K.; Kawano, S.; Tamura, Y.; Endo, T.; Umeda, M.; Hamachi, I. Organelle membrane-specific chemical labeling and dynamic imaging in living cells. *Nat. Chem. Biol.* **2020**, *16*, 1361−1367.
(41) Liang, G.; Ren, H.; Rao, J. A biocompatible condensation reaction for controlled assembly of nanostructures in living cells. *Nat. Chem.* **2010**, *2*, 54−60.
(42) Lock, L. L.; Reyes, C. D.; Zhang, P.; Cui, H. Tuning Cellular Uptake of Molecular Probes by Rational Design of Their Assembly into Supramolecular Nanoprobes. *J. Am. Chem. Soc.* **2016**, *138*, 3533−3540.
(43) Wang, F.; Gnewou, O.; Wang, S.; Osinski, T.; Zuo, X.; Egelman, E. H.; Conticello, V. P. Deterministic chaos in the self-assembly of $\beta$ sheet nanotubes from an amphipathic oligopeptide. *Matter* **2021**, *4*, 3217−3231.
(44) Shi, J.; Fichman, G.; Schneider, J. P. Enzymatic Control of the Conformational Landscape of Self-Assembling Peptides. *Angew. Chem., Int. Ed.* **2018**, *57*, 11188−11192.
(45) Lyles, M. M.; Gilbert, H. F. Catalysis of the oxidative folding of ribonuclease A by protein disulfide isomerase: pre-steady-state kinetics and the utilization of the oxidizing equivalents of the isomerase. *Biochemistry* **1991**, *30*, 619−625.





https://doi.org/10.1021/jacs.2c02238
*J. Am. Chem. Soc.* 2022, 144, 6709−6713